PLOS ONE

RESEARCH ARTICLE

Quantitative analysis of *HER2* mRNA expression by RNA *in situ* hybridization in canine mammary gland tumors: Comparison with immunohistochemistry analysis

Byung-Joon Seung, Seung-Hee Cho, Soo-Hyeon Kim, Ha-Young Lim, Jung-Hyang Sur*

Department of Veterinary Pathology, Small Animal Tumor Diagnostic Center, College of Veterinary Medicine, Konkuk University, Seoul, Republic of Korea

* jsur@konkuk.ac.kr

Citation: Seung B-J, Cho S-H, Kim S-H, Lim H-Y, Sur J-H (2020) Quantitative analysis of *HER2* mRNA expression by RNA *in situ* hybridization in canine mammary gland tumors: Comparison with immunohistochemistry analysis. PLoS ONE 15(2): e0229031. https://doi.org/10.1371/journal.pone.0229031

Editor: Douglas H. Thamm, Colorado State University, UNITED STATES

Received: October 1, 2019

Accepted: January 28, 2020

Published: February 14, 2020

Data Availability Statement: All relevant data are within the manuscript and its Supporting Information files.

Funding: This research was supported by the Bio & Medical Technology Development Program of the NRF funded by the Korean government, MSIT (2016M3A9B6903437) (JHS). And this paper was supported by Konkuk University Researcher Fund in 2019 (BJS, SHC, SHK). The funders had no role in study design, data collection and analysis,

Abstract

Spontaneously occurring canine mammary gland tumors share many features with human breast cancer, including biological behavior and histologic features. Compared to transgenic murine model, canine models have advantages including naturally occurring models of human diseases and cancer. In humans, breast cancer is divided into molecular subtypes based on ER, PR, and *HER2* expression. In contrast with humans, few studies have evaluated these subtypes in canine mammary gland tumors, including expression of *HER2*. *HER2* expression in canine mammary tissues has been further complicated by controversy regarding the antibody's specificity. This study aimed to investigate *c-erbB2* mRNA expression in retrospective formalin-fixed paraffin embedded samples, using RNA *in situ* hybridization with a novel quantitative assay and to compare this method with immunohistochemistry. Using 48 canine mammary tumor samples and 14 non-neoplastic canine mammary tissues, RNA *in situ* hybridization was performed with RNAscope® using a canine-specific target gene probe (*ERBB2*), and quantitative measurement was performed using the housekeeping gene (*POLR2A*) to calculate the target gene/housekeeping gene ratio. The ratio of *ERBB2/POLR2A* was quantified using open-source image analysis programs and compared with the immunohistochemistry results. A significant correlation was observed between the *HER2* immunohistochemistry score and *ERBB2/POLR2A* RNA *in situ* hybridization ($P < 0.001$). When the *HER2* immunohistochemistry score was 3+, significantly higher expression of *HER2* mRNA was observed by RNA *in situ* hybridization. Interestingly, *HER2* mRNA was also observed in non-neoplastic mammary tissues by RNA *in situ* hybridization. This assay potentially facilitates the reliable quantification of mRNA expression levels in retrospective formalin-fixed paraffin-embedded samples. Further studies are required to elucidate the role of *HER2* in canine mammary gland tumors and to implement clinical trials in dogs.

decision to publish, or preparation of the manuscript.

Competing interests: The authors have declared that no competing interests exist.

Introduction

Spontaneously occurring canine mammary gland tumors (CMTs) are the most common tumor type in intact female dogs [1, 2]. CMTs in dogs share many epidemiological, biological, and clinical features with human breast cancer including their biological behavior and histologic features [3]. The few actively used prognostic factors for CMTs include histopathological classification and histologic grading, which have now been modified to model the criteria for human breast cancer [4–6]. Unlike that in humans, in dogs, surgery is the main treatment option for CMTs, and other systemic treatment options are limited to the research stage because they have not been sufficiently studied [7, 8]. Therefore, further studies are required to provide a basis for treatments including chemotherapy for CMTs.

In humans, breast cancer exhibits well-established intrinsic subtypes (luminal A, luminal B, *HER2*-enriched, and basal-like), facilitating accurate diagnosis and effective treatment [9]. Among these, the *HER2*-enriched subtype, accounting for approximately 15–25% of breast cancer cases, benefits from *HER2*-targeted chemotherapy using trastuzumab in humans [10–12]. In human breast cancer, *HER2* status was commonly determined using Immunohistochemistry (IHC) or fluorescence *in situ* hybridization [13]. Few studies, however, have evaluated the molecular subtypes of CMTs by immunohistochemistry, including *HER2* expression, and have revealed inconsistent results [14, 15]. Ahern *et al*. reported that *HER2* mRNA levels were lower in benign CMTs than in malignant CMTs through hybridization of total polysomal RNA with the human *c-erbB-2* probe [16]. However, Peña *et al*. reported discordant results in subsequent IHC studies [17]. Additionally, studies of *HER2* expression in CMTs using IHC with an FDA-approved anti-*HER2* polyclonal antibody (A0485, Dako, Glostrup, Denmark) revealed differences in the expression patterns and non-specific cytoplasmic staining patterns in accordance with the criteria for human breast cancer [18, 19].

RNAscope is a recently developed method for RNA *in situ* hybridization (RNA-ISH), using a novel probe design and unique amplification system to amplify target-specific signals without background interference [20]. This RNA-ISH technique can be used to rapidly detect RNA with high sensitivity in formalin-fixed paraffin-embedded (FFPE) tissues [20].

In this study, we investigated *HER2* mRNA levels by assessing *c-erbB2* expression in CMTs using RNA-ISH with a new quantitative assay method in retrospective FFPE CMTs samples. We assessed *HER2* protein levels in CMTs by immunohistochemistry using the FDA-approved anti-*HER2* antibody and compared the results with those obtained using RNA-ISH.

Materials and methods

Ethical statement

The protocol for tissue sampling was approved by the Institutional Animal Care and Use Committee of Konkuk University (KU16106, KU17162, and KU18168). Tissue samples were acquired as routine diagnostic procedures from privately owned pet dogs via private veterinary hospitals with informed consent from the owner.

Case selection and histopathological analysis

Forty-eight CMT samples and 14 non-neoplastic canine mammary tissue samples that were suspected tumors but diagnosed as mammary gland hyperplasia were selected from the archived FFPE database from 2017 to 2019 at the Department of Veterinary Pathology, Konkuk University. Simple random sampling was performed for CMT samples yielding *HER2* IHC data (available from our previous data descriptor [21] and validation studies) with complete clinical data. During RNA-ISH, tissue samples not suitable for analysis were excluded

(describe in detail below). To prevent unequal distribution of the *HER2* IHC score in malignant CMTs, additional selections were performed until each *HER2* IHC score (1+, 2+, and 3+) was obtained from at least 10 samples. Ultimately, 38 FFPE CMT specimens were included in our previous data descriptor article [21].

Forty-three dogs were intact females and 19 dogs were spayed females. The breeds included Maltese (n = 20), Shih-Tzu (n = 10), Mixed (n = 9), Poodle (n = 8), Schnauzer (n = 5), Yorkshire Terrier (n = 3), Cocker Spaniel (n = 2), Pomeranian (n = 2), English sheepdog (n = 1), Miniature Pinscher (n = 1) and Pekingese (n = 1). The age range of the dogs was 2–16 years [mean ± standard deviation (SD): 11.15 ± 3.02]. The detailed regarding sample characteristics are listed in S1 Table.

For histological examination, 4-μm-thick sections from FFPE tissues were stained with hematoxylin and eosin and diagnosed by two researchers (B.J.S. and J.H.S.). The histological subtype of each sample was categorized based on the World Health Organization classification for CMTs [4]. The histological grade was assessed based on the criteria described by Peña *et al.* [6]. Lymphatic invasion, defined as infiltration of tumor cells in lymphatic vessels, was also evaluated.

Immunohistochemistry

To evaluate the expression of *HER2* protein, 4-μm-thick sections from FFPE tissues were used. Because of intra-tumor heterogeneity, serial sections were used for IHC and ISH experiments. IHC was performed as previously described with the polyclonal anti-human c-erbB-2 oncoprotein antibody (Dako) [22]. Control slides known to be positive for *HER2* were used as positive controls. Isotype-matched immunoglobulins were used as negative controls. *HER2* staining was scored on the basis of the guidelines of the American Society of Clinical Oncology/College of American Pathologists (0: No staining is observed or incomplete membrane staining that is faintly perceptible within $\leq$10% of epithelial tumor cells; 1+: Incomplete membrane staining that is faintly perceptible and within >10% of epithelial tumor cells; 2+: Weak to moderate complete membrane staining within >10% of tumor cells or complete intense membrane staining within $\leq$10% of tumor cells; and 3+: Intense complete membrane staining within >10% of tumor cells) [23]. According to human criteria, the observation of cytoplasmic staining (described by Burrai et al [19]) is non-specific, and the evaluation by B.J.S. was focused on a complete membranous staining pattern between score 1+ and 2+ and staining intensity between score 2+ and 3+. For ambiguous samples, a consensus was reached by the two researchers (B.J.S. and J.H.S.).

RNA *in situ* hybridization

RNA-ISH was performed for FFPE tissues using the RNAscope duplex assay (Advanced Cell Diagnostics, Hayward, CA, USA). Because the RNA quality of FFPE tissues retrieved from storage archives showed variation following the storage period and fixation process [24], we performed quantitative analysis through dual detection of target genes and housekeeping genes in one section and determined the target gene/housekeeping gene ratio. To detect the target mRNA (*HER2*) in individual epithelial cells, we used an *ERBB2* target probe (Cat. No.432411, Advanced Cell Diagnostics). A *POLR2A* probe (Cat. No.479111-C2, Advanced Cell Diagnostics) was used as a housekeeping gene following the manufacturer's recommendations for canine tissue. GenBank accession numbers and probe regions are as follows: *ERBB2* (GenBank, NM_001003217.1; probe region, 1585–2823) and *POLR2A* (GenBank XM_852751.3; probe region, 1846–2924). The procedure was manually carried out in accordance with the manufacturer's instructions. Briefly, 4-μm-thick sections (serial sections with IHC slides) were baked for 1 h at 60˚C in an oven, deparaffinized in xylene twice for 5 min

each, and dehydrated in 100% ethanol twice for 2 min each. After the sections were air-dried, they were treated with RNAscope hydrogen peroxide solution (Cat. No. 322330, Advanced Cell Diagnostics) for 10 min at room temperature and washed with distilled water. The sections were incubated in target retrieval reagent (Cat. No.322000, Advanced Cell Diagnostics) maintained at a boiling temperature (93–98˚C) using a hot plate for 15 min, and then washed with distilled water. A hydrophobic barrier was drawn around the samples using an Immedge hydrophobic barrier pen (Cat. No. H-4000, Vector Laboratories, Burlingame, CA, USA). Each section was treated with Protease plus (Cat. No.322330, Advanced Cell Diagnostics) reagents for 30 min at 40˚C in a HybEZ hybridization oven (Advanced Cell Diagnostics). The sections were then incubated for 2 h at 40˚C in a HybEZ hybridization oven using probes mixed with an *ERBB2* probe (C1-Blue) and *POLR2A* probe (C2-red) at a 50:1 ratio. The slides were repeatedly washed twice with wash buffer reagent (Cat. No.310091, Advanced Cell Diagnostics) after each amplification step using RNAscope 2.5 HD Duplex Detection Reagent (Cat. No.322500, Advanced Cell Diagnostics). Chromogenic detection was carried out using fast red (C2), followed by DAB chromogenic (C1) detection for 10 min at room temperature. Counterstaining was performed using 50% Gill's hematoxylin. The bacterial gene DapB probe was used as a negative control at the same mixing ratio (50:1) for the C1 and C2 probe.

Evaluation of RNA-ISH results

RNA-ISH images were acquired (by B.J.S.) from five representative regions corresponding to the IHC scores and the histological diagnosis at 400× magnification for each sample. Digital images were acquired using an Olympus BX51 microscope (Tokyo, Japan) and Image transfer software (Olympus). In the RNA-ISH results, blue dots (*HER2* mRNA) and red dots (*POLR2A* mRNA) were measured to determine the average ratios (*ERBB2*/*POLR2A* ISH ratio) for five representative images per sample. We used two open-source image analysis programs (Fiji [25] and ICY [26]) to analyze the images obtained after RNA-ISH experiments. First, the images were converted using the "Dichromacy > Tritanope" filters in Fiji to select blue signals against hematoxylin counterstaining. After selecting regions of interest (ROI) containing only epithelial regions in the filtered image (400× magnification; by B.J.S.), using ICY program, blue dots (*ERBB2* mRNA) were measured using dark spot detection mode in the spot detector of ICY. To measure the red dots, Tritanope-filtered images were converted to a CIELAB (RGB to CIELAB) and 'a' channel images were acquired as jpg files. Red dots (*POLR2A* mRNA) were quantified using bright spot detection mode in the spot detector of ICY. In some tissue sections, the red channel (housekeeping gene) was not successful owing to RNA degradation or observed with high background of fast red may be due to endogenous alkaline phosphatase. These samples were excluded from the analysis. The quantification procedures are illustrated in Figs 1 and 2. And quantification procedure also deposited at protocols.io (dx.doi.org/10.17504/protocols.io.badcia2w).

Statistical analysis

The *ERBB2*/*POLR2A* ISH ratio and *HER2* IHC score were compared by the Kruskal–Wallis test, followed by post-hoc analysis with Bonferroni correction. Comparisons between ISH ratio and three groups were also performed using Kruskal-Wallis test and comparisons between ISH ratio and two groups were performed using Mann–Whitney U test. Categorical variables were analyzed using Fisher's exact test. Statistical analyses were performed using SPSS version 24.0 software for Windows (SPSS, Inc., Chicago, IL, USA). Values were considered as significant when $P < 0.05$.

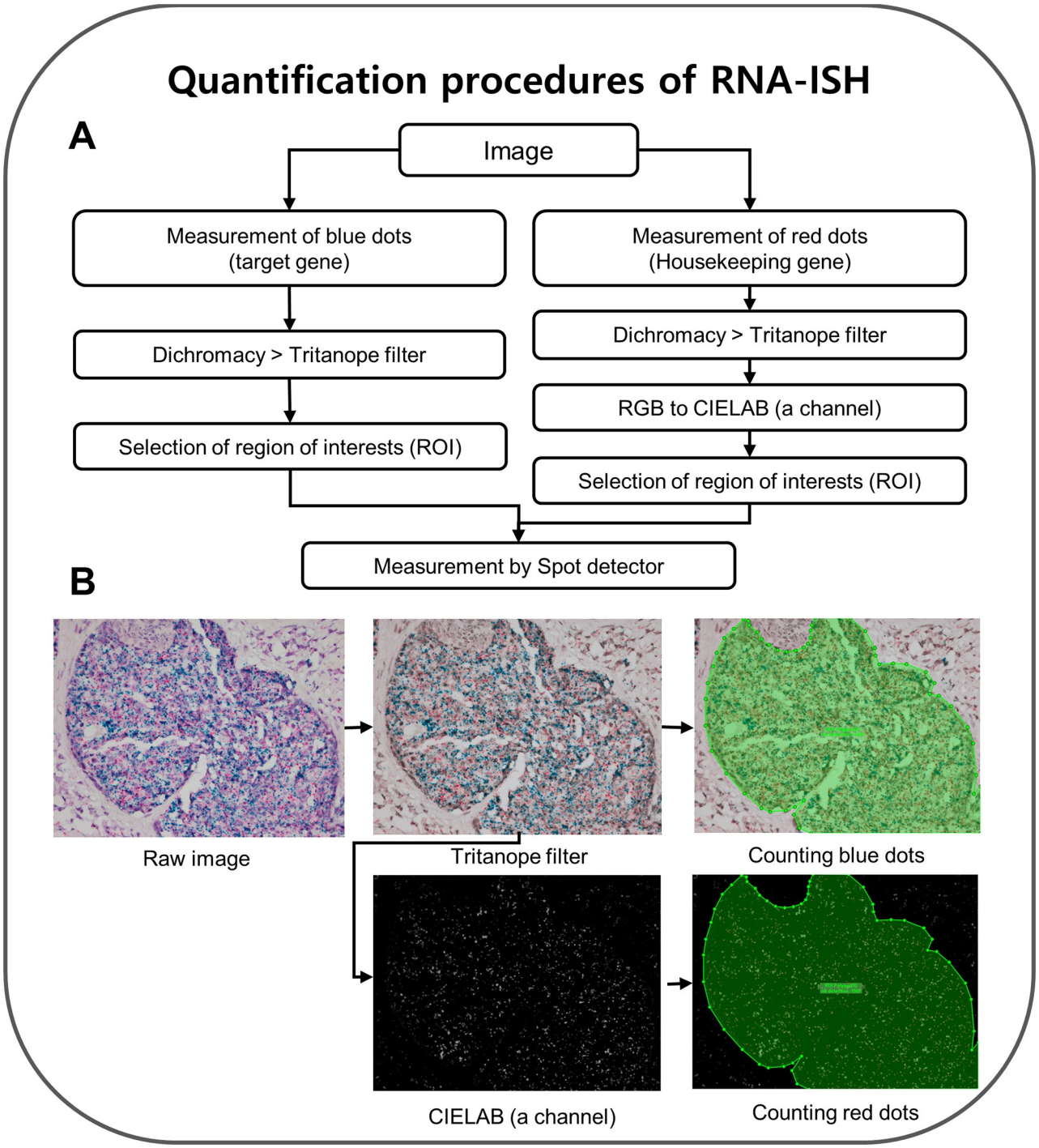

Fig 1. Workflow of quantification procedures of RNA-ISH. (A) Flow chart for quantitative analysis of RNA-ISH images. (B) Representative RNA-ISH raw images are converted using each filter, and quantitative analysis is automatically performed using the spot detection software.

https://doi.org/10.1371/journal.pone.0229031.g001

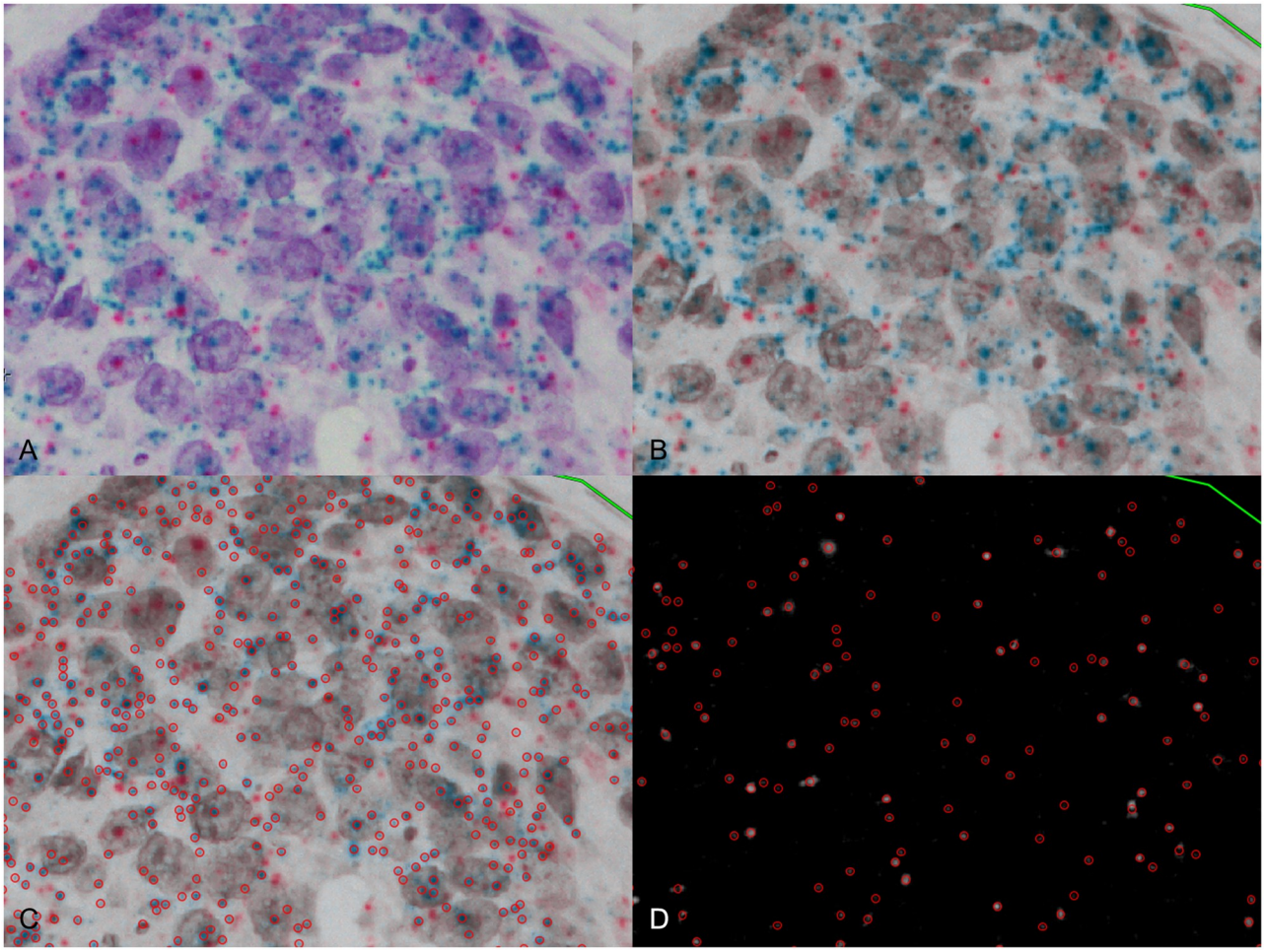

Fig 2. Example of analyzing RNA-ISH images. (A) Original image of RNA-ISH. Blue dots (*HER2*) and red dots (*POLR2A*) were observed. (B) Blue dots and red dots were observed in Tritanope filtered image. (C) Blue dots are recognized and enumerated by spot detector of open-source program. (D) Red dots are recognized and enumerated by spot detector of open-source program.

https://doi.org/10.1371/journal.pone.0229031.g002

Results

Histology

Histologically, samples were classified as malignant (n = 42), benign (n = 6) and hyperplasia (n = 14). The histological subtypes of CMTs were classified as simple adenoma (n = 4), complex adenoma (n = 2), simple carcinoma (n = 26), and complex carcinoma (n = 16). The histological grade of malignant CMTs included grade 1 (n = 23), grade 2 (n = 9), and grade 3 (n = 10). Six cases of malignant CMTs exhibited evidence of lymphatic invasion.

HER2 protein expression

Among the 62 CMT and non-neoplastic tissue samples, the *HER2* scores were classified as 1+ (n = 20), 2+ (n = 24), and 3+ (n = 18). In malignant CMT samples, 15 cases of carcinoma (8 simple and 7 complex) were scored as 1+, 15 cases of carcinoma (10 simple and 5 complex) were scored as 2+, and 12 cases of carcinoma (8 simple and 4 complex) were scored as 3+, with intense and complete immunoreactivity observed in more than 10% of epithelial tumor cells. In benign CMT samples, 2 cases of adenoma (2 complex) were scored as 1+, 3 cases of

Table 1. The *HER2* IHC score according to histological subtype of samples.

	Histological subtype				
	Non-neoplastic tissue	Benign CMT		Malignant CMT	
	Mammary gland hyperplasia	Simple adenoma	Complex adenoma	Simple carcinoma	Complex carcinoma
HER2 IHC Score	n/total (%)	n/total (%)	n/total (%)	n/total (%)	n/total (%)
0	0/0 (0%)	0/0 (0%)	0/0 (0%)	0/0 (0%)	0/0 (0%)
1+	3/20 (15.0%)	0/20 (0%)	2/20 (10.0%)	8/20 (40.0%)	7/20 (35.0%)
2+	6/24 (25.0%)	3/24 (12.5%)	0/24 (0%)	10/24 (41.7%)	5/24 (20.8%)
3+	5/18 (27.8%)	1/18 (5.6%)	0/18 (0%)	8/18 (44.4%)	4/18 (22.2%)

IHC, Immunohistochemistry; CMT, Canine mammary gland tumor

https://doi.org/10.1371/journal.pone.0229031.t001

adenoma (3 simple) were scored as 2+, and 1 case of adenoma (1 simple) was scored as 3+. In mammary gland hyperplasia samples, 3 cases of samples were scored as 1+, 6 cases of samples were scored as 2+, and 5 cases of samples were scored as 3+. The results of the *HER2* IHC score according to histological subtype were summarized in Table 1. In line with other studies [18, 19, 27], we also observed the cytoplasmic staining patterns of *HER2* in CMTs, and only membranous staining patterns were evaluated in this study. *HER2* expression was also observed in adjacent normal or hyperplastic mammary glands in CMTs and non-neoplastic tissues.

HER2 mRNA expression

HER2 mRNA expression in canine mammary gland tissue was investigated by the RNA-ISH method. Because retrospective FFPE tissue samples from archives contain different amounts of RNA, the ratio between *ERBB2* and the reference gene (*POLR2A*) was determined. The range of the *ERBB2*/*POLR2A* ISH ratio was 1.521–4.952 [mean ± standard deviation (SD): 3.079 ± 0.743]. The association between the *HER2* (RNA-ISH results and IHC results) and parameters including the histological diagnosis, histological subtype, malignancy, histological grade, and presence of lymphatic invasion are summarized in Tables 2 and 3. *HER2* mRNA dots were primarily observed in epithelial regions of the tumor. Although *POLR2A* reference mRNA dots were observed in both the epithelial and stromal regions, only the epithelial regions were counted upon selecting the ROI. In samples with upregulated *HER2* mRNA, the mRNA dots were observed as clusters and dense clusters of *HER2* mRNA signals were counted less than actual mRNA expression in some 3+ score cases. (S1 Fig).

Comparison of *HER2* expression by RNA-ISH and immunohistochemistry

To compare *HER2* IHC scores with the RNA-ISH results, RNA-ISH images were acquired in representative regions corresponding to those used to determine IHC scores. Expression of *HER2* mRNA dots was observed in the region showing a strong membrane staining pattern in IHC (Fig 3A–3D). Furthermore, the expression of *HER2* mRNA dots was observed in non-neoplastic lesions (Fig 4A and 4B). In some cases, the expression of *HER2* mRNA dots was observed in the area around the tumor where staining pattern was observed in the adjacent normal mammary gland by IHC (Fig 4C and 4D). A significant correlation between the *HER2* IHC score and *ERBB2/POLR2A* ISH ratio was observed ($P < 0.000$) in canine mammary tissues (Fig 5A and 5B). In addition, significant differences were observed between the 1+ score vs. 3+ score (Bonferroni-corrected P value < 0.001) and 2+ score vs. 3+ score (Bonferroni-corrected P value = 0.002) (Fig 5A). When the *HER2* IHC score was 3+, significantly higher expression of

Table 2. Association between the *ERBB2/POLR2A* ISH ratio and parameter including malignancy, histological subtype, histological grade, presence of lymphatic invasion, and *HER2* IHC score.

	ERBB2/POLR2A ISH ratio (Mean ± SD)	*P*-value
Histological diagnosis [a]		
Non-neoplastic lesion (n = 14)	3.33 ± 0.80	0.301
Benign (n = 6)	2.78 ± 0.21	
Malignant (n = 42)	3.04 ± 0.76	
Histological subtype [b]		
Simple type (n = 30)	3.02 ± 0.77	0.983
Complex type (n = 18)	2.98 ± 0.64	
Histological grade [a]		
Grade 1 (n = 23)	2.90 ± 0.59	0.174
Grade 2 (n = 9)	2.89 ± 0.89	
Grade 3 (n = 10)	3.47 ± 0.90	
Lymphatic invasion [b]		
Absent (n = 36)	2.99 ± 0.72	0.428
Present (n = 6)	3.30 ± 0.97	
***HER2* IHC score in malignant CMTs** [a]		
1+ (n = 15)	2.43 ± 0.56	**<0. 001**
2+ (n = 15)	3.01 ± 0.40	
3+ (n = 12)	3.82 ± 0.62	
***HER2* IHC score in canine mammary tissues** [a]		
1+ (n = 20)	2.51 ± 0.52	**<0. 001**
2+ (n = 24)	3.00 ± 0.50	
3+ (n = 18)	3.81 ± 0.62	
***HER2* membranous staining pattern in malignant CMTs** [b]		
Incomplete (1+) (n = 15)	2.43 ± 0.56	**< 0.001**
Complete (2+ and 3+) (n = 27)	3.37 ± 0.65	
***HER2* membranous staining pattern in canine mammary tissues** [b]		
Incomplete (1+) (n = 20)	2.51 ± 0.52	**< 0.001**
Complete (2+ and 3+) (n = 42)	3.35 ± 0.68	

IHC, Immunohistochemistry; CMTs, Canine mammary gland tumors; SD, Standard deviation

[a] Kruskal-Wallis test

[b] Mann-Whitney test

https://doi.org/10.1371/journal.pone.0229031.t002

HER2 mRNA was observed by RNA-ISH. Significant differences were observed based on complete membranous staining pattern between 1+ score (incomplete membranous staining) and 2+, 3+ score (complete membranous staining) ($P < 0.001$) (Fig 5B). No significant differences were observed in the *HER2* IHC score and RNA-ISH results for clinicopathological parameters.

Discussion

In humans, breast cancers with *HER2* overexpression display aggressive behavior and are associated with reduced patient survival [28, 29]. Anti-*HER2* therapies including trastuzumab, a monoclonal antibody targeting the extracellular domain of *HER2*, has improved treatment outcomes [12, 30]. *HER2* protein has gained increasing attention in veterinary oncology and was recently investigated in dogs. However, studies on *HER2* expression in CMTs using human anti-*HER2* antibody, have shown variable results [14, 15, 31]. The specificity of human

Table 3. Association between *HER2* IHC score and parameter including histological diagnosis, histological grade, presence of lymphatic invasion.

	HER2 1+ (IHC) (Incomplete membranous staining)	*HER2* 2+ and 3+ (IHC) (Complete membranous staining)	*P*-value
	n/total (%)	n/total (%)	
Histological Diagnosis [a]			
Non-neoplastic (n = 14)	3/14 (21.4%)	11/14 (78.6%)	0.697
Benign CMTs (n = 6)	2/6 (33.3%)	4/6 (66.7%)	
Malignant CMTs (n = 42)	15/42 (35.7%)	27/42 (64.3%)	
Histological grade [a]			
Grade 1 (n = 23)	8/23 (34.8%)	15/23 (65.2%)	0.317
Grade 2 (n = 9)	5/9 (55.6%)	4/9 (44.4%)	
Grade 3 (n = 10)	2/10 (20.0%)	8/10 (80.0%)	
Lymphatic invasion [a]			
Absent (n = 36)	14/36 (38.9%)	22/36 (61.1%)	0.395
Present (n = 6)	1/6 (16.7%)	5/6 (83.3%)	

IHC, Immunohistochemistry

[a] Fisher's exact test

https://doi.org/10.1371/journal.pone.0229031.t003

anti-*HER2* antibody (Dako A0485) for detecting *HER2* in canine tissues remains controversial. One study showed no evidence of its specificity in canine tissues by western blotting and subsequent mass spectrometric analysis [19], while another recent study showed the cross-reactivity of the human anti-*HER2* antibody in canine tissue by western blotting [27].

Furthermore, the present results displayed cytoplasmic immunoreactivity in tumor cells and non-neoplastic cells, similar to the results of some previous studies [18, 19, 27]. As this cytoplasmic immunoreactivity is considered non-specific in accordance with human criteria, we limited our analysis to membranous immunoreactivity. Previous studies [19, 32] have shown that mRNA and IHC levels are not completely correlated in CMTs, probably owing to post-translational events [33].

In our study, however, *HER2* mRNA levels were high in IHC samples with strong complete membranous staining pattern (3+), and a significant correlation was observed between the IHC score and RNA-ISH results. Furthermore, similar expression pattern was observed in high power field images (Figs 3 and 4) in which left and right sides were expressed differently due to intra-tumor heterogeneity [34]. This discrepancy in our results relative to previous results may have occurred by using consecutive sections and restricting RNA-ISH analysis of gene expression to epithelial regions and matching the IHC scores to prevent intra-tumor heterogeneity. Furthermore, this *in situ* detection technology (RNA-ISH) is superior to RT-PCR, which depends on an admixture of cells with a potentially low content of malignant epithelial cells. Our results are consistent with those of a previous study that analyzed *HER2* mRNA expression in human breast cancer by RT-PCR and RNA-ISH in parallel [35]. Significant differences in the RNA-ISH results were also observed depending on complete membranous staining pattern. Although the specificity of the anti-*HER2* antibody is controversial, the present results reduced the likelihood of nonspecific findings with antibodies during IHC by morphologically confirming mRNA expression directly in tissue and comparing it with IHC results. And thus, IHC method may be used as a complement to assess the *HER2* status determined from membrane staining pattern (RNA-ISH method is more specific).

To confirm the association between *HER2* expression and its prognosis in CMTs, we assessed the available clinical parameters. However, no significant correlation was observed between the *HER2* status (mRNA and protein levels) and clinical parameters (malignancy,

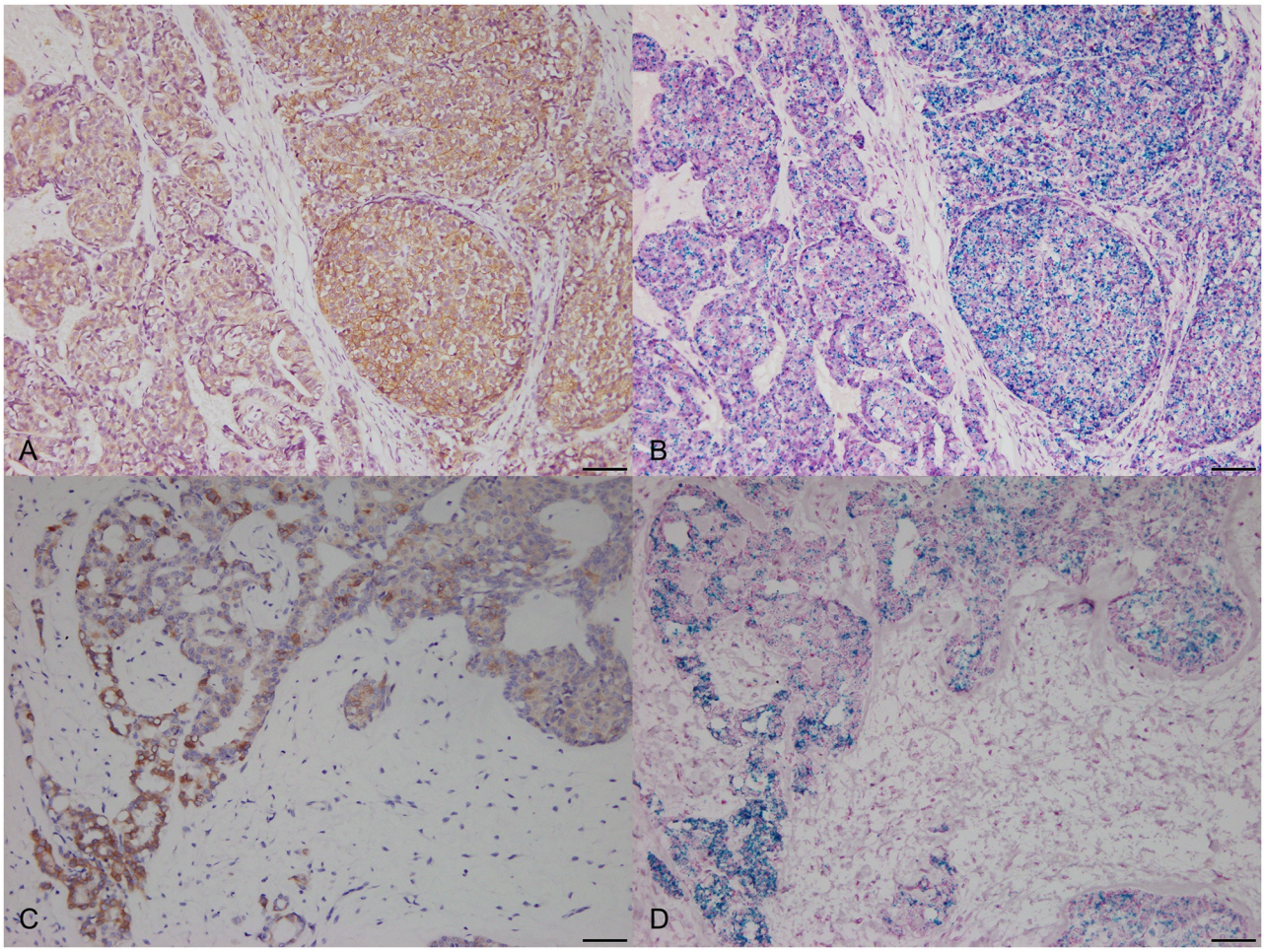

Fig 3. *HER2* expression in adjacent serial section of canine mammary gland tissues. (A) Strong membranous staining pattern was observed in the right side of images by IHC 200×, bar = 50 μm. (B) Expression of *HER2* mRNA dots was observed in corresponding regions of adjacent serial section to Fig 3A by RNA-ISH, 200×, bar = 50 μm. (C) Strong membranous staining pattern staining pattern was observed in the bottom-left side of images by IHC 200×, bar = 50 μm. (D) Expression of *HER2* mRNA dots was observed in corresponding regions adjacent serial sections to Fig 3C by RNA-ISH, 200×, bar = 50 μm.

https://doi.org/10.1371/journal.pone.0229031.g003

histological subtype, histological grade, lymphatic invasion). This is consistent with the results of previous studies showing that *HER2* is not associated with poor prognostic factors in CMTs [18, 36, 37]. Additionally, present study revealed that HER2 is also expressed in non-neoplastic mammary gland tissues. This is a distinct characteristic from that of human breast cancer, suggesting prospects for future study from the viewpoint of comparative medical research. Recently, lower prevalence of *ERBB2* copy number variant was observed in HER2 protein overexpressing canine urothelial carcinoma [38]. In present study, we did not confirm the *HER2* amplification status in canine mammary tissues, which is correlated with *HER2* overexpression in human breast cancer, and only observed mRNA and protein levels; thus, further studies are needed to determine expression of *HER2* mRNA is due to gene amplification or other mechanism.

This study shows the use of quantitative RNA-ISH. RNA-ISH technology with RNAscope has already been used to for human breast cancer to determine *HER2* mRNA levels in equivocal cases (IHC 2+ or a Fluorescence ISH ratio of 1.8 to 2.2) and has displayed better performance

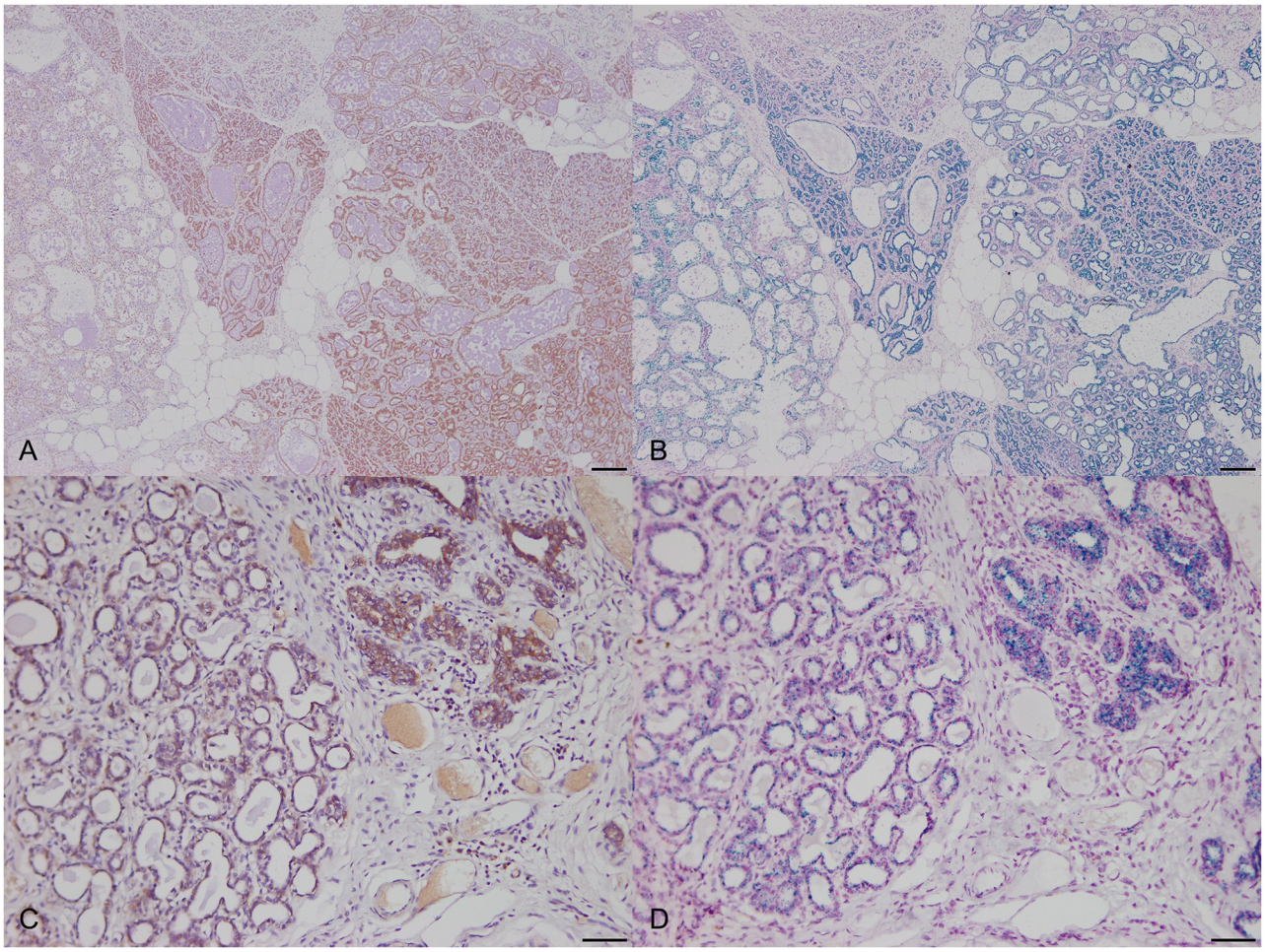

Fig 4. *HER2* expression in adjacent serial section of non-neoplastic regions. (A) Strong membrane staining pattern (3+) in right sides of mammary gland hyperplasia samples by IHC, 40×, bar = 200 μm. (B) Expression of *HER2* mRNA dots was observed in the section of serial to Fig 4A by RNA-ISH, 40×, bar = 200 μm. (C) Moderate *HER2* staining was observed in the adjacent normal mammary gland in CMT by IHC, 200×, bar = 50 μm. (D) Expression of *HER2* mRNA dots was observed in the section of serial to Fig 4C by RNA-ISH, 200×, bar = 50 μm.

https://doi.org/10.1371/journal.pone.0229031.g004

than that by qPCR [35]. In retrospective studies, RNA preservation may vary between FFPE samples from archives; hence, we used a dual detection RNA-ISH method to compare with housekeeping genes, unlike that in previous studies. This assay method has been primarily used in fluorescence ISH to confirm *HER2* gene amplification by *HER2* to chromosome 17 ratio in breast cancer [39]. In addition, manual enumeration of dots is difficult; hence, to enumerate the dots to determine the target gene/housekeeping gene ratio, we developed an automated measurement protocol using open-source programs. The method displayed adequate performance without human subjectivity in recognizing dots. Although dense clusters of dots tended to be enumerated at lower levels than the actual expression levels, our experimental groups yielded significant results. The present method of *in situ* analysis of RNA in tissues is potentially applicable in studies using retrospective FFPE samples. Furthermore, the RNA-ISH method may be used to supplement existing IHC methods if the antibody is not adequately sensitive or if no antibodies are available (newly discovered gene signatures studies).

Compared to the use of transgenic murine models, the use of naturally occurring canine models of human diseases for translational research has benefits for dogs and for study cancer

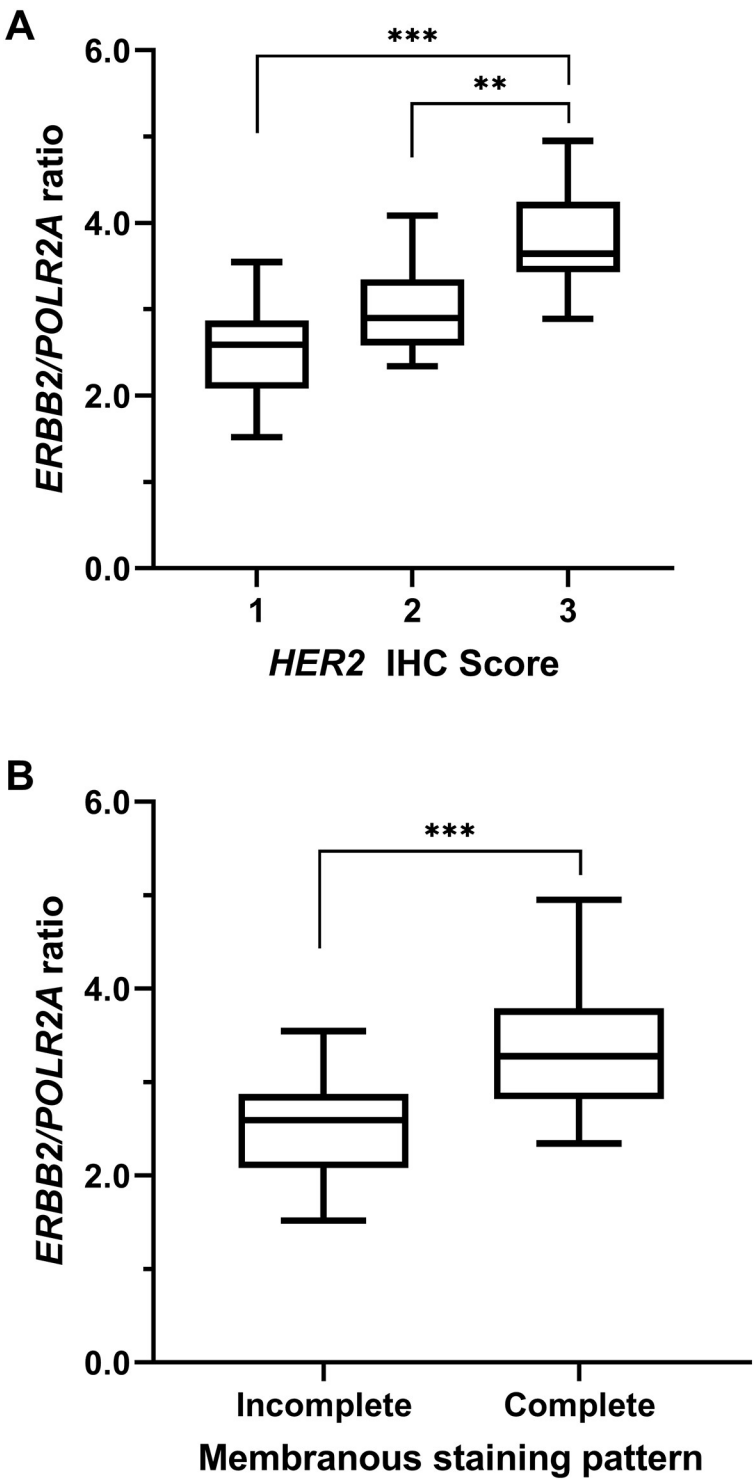

Fig 5. Comparison of the *ERBB2/POLR2A* ISH ratio according to *HER2* IHC score in canine mammary tissues. A significant correlation between the *HER2* IHC score and *ERBB2/POLR2A* ISH ratio was observed (**, $P < 0.01$; ***, $P < 0.001$).

https://doi.org/10.1371/journal.pone.0229031.g005

in humans [40]. Using canine models to evaluate human diseases is advantageous because they exhibit naturally occurring cancer, clinical similarities, high incidences, and shorter lifespans than humans [41, 42]. Recently, *HER2*-targeted cancer immunotherapy using recombinant *Listeria monocytogenes*, which expresses a chimeric human *HER2*/neu construct, was shown to prolong the overall survival and reduce metastasis rates in canine models of pediatric osteosarcomas [43]. Additionally, small-molecule tyrosine kinase inhibitor (lapatinib) of *HER2*, which may cross-react between species, exerted anti-tumor effects in canine transitional cell carcinoma cell lines [44]. Such comparative studies using canine models may not only facilitate individual therapeutic methods for dogs but are also applicable in understanding the pathogenesis of human cancers.

Conclusions

In this study, we assessed *HER2* mRNA levels in CMTs using RNA-ISH and observed a correlation with the *HER2* immunohistochemistry score. We developed an automated, quantitative dual staining RNA-ISH method to evaluate *HER2* expression relative to that of a housekeeping gene. This assay potentially allows for reliable quantification of mRNA expression levels in retrospective FFPE samples. Because no correlation was identified in this study between *HER2* expression and clinical parameters, further studies are needed to clarify if there is a role of *HER2* in the pathogenesis of CMTs.

Supporting information

S1 Table. Clinical information of the samples. The avaialbe clinical information of 62 samples are listed.
(XLSX)

S1 Fig. Example image of dense clusters of *HER2* mRNA dots tended to be enumerated at lower levels than the actual expression levels.
(TIF)

Acknowledgments

We thank Ms. E.M. Yu for her excellent technical assistance. This report represents a part of the PhD thesis by Byung-Joon Seung.

Author Contributions

Conceptualization: Byung-Joon Seung, Jung-Hyang Sur.

Data curation: Byung-Joon Seung, Seung-Hee Cho, Soo-Hyeon Kim, Ha-Young Lim.

Formal analysis: Byung-Joon Seung, Seung-Hee Cho, Soo-Hyeon Kim, Ha-Young Lim.

Funding acquisition: Jung-Hyang Sur.

Investigation: Byung-Joon Seung, Seung-Hee Cho, Soo-Hyeon Kim, Ha-Young Lim, Jung-Hyang Sur.

Methodology: Byung-Joon Seung.

Project administration: Jung-Hyang Sur.

Resources: Jung-Hyang Sur.

Validation: Byung-Joon Seung.

Writing – original draft: Byung-Joon Seung.

Writing – review & editing: Byung-Joon Seung, Jung-Hyang Sur.

References

1. Sorenmo K. Canine mammary gland tumors. Vet Clin North Am Small Anim Pract. 2003; 33(3):573–96. https://doi.org/10.1016/s0195-5616(03)00020-2 PMID: 12852237
2. Goldschmidt MH, Peña L, Zappulli V. Tumors of the mammary gland. In: Meuten DJ, editor. Tumors in Domestic Animals. 5th ed. Ames, Iowa: John Wiley & Sons; 2017. p. 723–765.
3. Pinho SS, Carvalho S, Cabral J, Reis CA, Gärtner F. Canine tumors: a spontaneous animal model of human carcinogenesis. Transl Res. 2012; 159(3):165–72. https://doi.org/10.1016/j.trsl.2011.11.005 PMID: 22340765
4. Misdorp W, Else RW, Hellmen E, Lipscomb TP. Histologic classification of mammary tumors of the dog and the cat. In: World Health Organization international histological classification of tumors of domestic animals. 2nd ed. Vol 7. Washington, DC: Armed Force Institute of Pathol; 1999. p. 11–29.
5. Elston CW, Ellis IO. Pathological prognostic factors in breast cancer. I. The value of histological grade in breast cancer: experience from a large study with long-term follow-up. Histopathology. 1991; 19:403–10. https://doi.org/10.1111/j.1365-2559.1991.tb00229.x PMID: 1757079
6. Peña L, De Andrés PJ, Clemente M, Cuesta P, Perez-Alenza MD. Prognostic value of histological grading in noninflammatory canine mammary carcinomas in a prospective study with two-year follow-up: relationship with clinical and histological characteristics. Vet Pathol. 2013; 50(1):94–105. https://doi.org/10.1177/0300985812447830 PMID: 22688585
7. Novosad CA. Principles of treatment for mammary gland tumors. Clin Tech Small Anim Pract. 2003; 18 (2):107–9. PMID: 12831071
8. Lana S, Rutteman GR, Withrow SJ. Tumors of the mammary gland. In: Withrow SJ, Vail DM, editors. Withrow and Macewen's small animal clinical oncology. 4th ed. St.Louis: Saunders Elsevier; 2007. p. 619–36.
9. Parker JS, Mullins M, Cheang MC, Leung S, Voduc D, Vickery T, et al. Supervised risk predictor of breast cancer based on intrinsic subtypes. J Clin Oncol. 2009; 27(8):1160–7. https://doi.org/10.1200/JCO.2008.18.1370 PMID: 19204204
10. Llombart-Cussac A, Cortés J, Paré L, Galván P, Bermejo B, Martínez N, et al. HER2-enriched subtype as a predictor of pathological complete response following trastuzumab and lapatinib without chemotherapy in early-stage HER2-positive breast cancer (PAMELA): an open-label, single-group, multicentre, phase 2 trial. Lancet Oncol. 2017; 18(4):545–54. https://doi.org/10.1016/S1470-2045(17)30021-9 PMID: 28238593
11. Piccart-Gebhart MJ, Procter M, Leyland-Jones B, Goldhirsch A, Untch M, Smith I, et al. Trastuzumab after adjuvant chemotherapy in HER2-positive breast cancer. N Engl J Med. 2005; 353(16):1659–72. https://doi.org/10.1056/NEJMoa052306 PMID: 16236737
12. Slamon DJ, Leyland-Jones B, Shak S, Fuchs H, Paton V, Bajamonde A, et al. Use of chemotherapy plus a monoclonal antibody against HER2 for metastatic breast cancer that overexpresses HER2. N Engl J Med. 2001; 344(11):783–92. https://doi.org/10.1056/NEJM200103153441101 PMID: 11248153
13. Perez EA, Cortés J, Gonzalez-Angulo AM, Bartlett JM. HER2 testing: current status and future directions. Cancer Treat Rev. 2014; 40(2):276–84. https://doi.org/10.1016/j.ctrv.2013.09.001 PMID: 24080154
14. Kim NH, Lim HY, Im KS, Kim JH, Sur JH. Identification of triple-negative and basal-like canine mammary carcinomas using four basal markers. J Comp Pathol. 2013; 148(4):298–306. https://doi.org/10.1016/j.jcpa.2012.08.009 PMID: 23079102
15. Gama A, Alves A, Schmitt F. Identification of molecular phenotypes in canine mammary carcinomas with clinical implications: application of the human classification. Virchows Arch. 2008; 453(2):123–32. https://doi.org/10.1007/s00428-008-0644-3 PMID: 18677512
16. Ahern TE, Bird RC, Bird AE, Wolfe LG. Expression of the oncogene c-erbB-2 in canine mammary cancers and tumor-derived cell lines. Am J Vet Res. 1996; 57(5):693–6. PMID: 8723884
17. Peña L, Gama A, Goldschmidt MH, Abadie J, Benazzi C, Castagnaro M, et al. Canine mammary tumors: a review and consensus of standard guidelines on epithelial and myoepithelial phenotype markers, HER2, and hormone receptor assessment using immunohistochemistry. Vet Pathol. 2014; 51 (1):127–45. https://doi.org/10.1177/0300985813509388 PMID: 24227007
18. Ressel L, Puleio R, Loria GR, Vannozzi I, Millanta F, Caracappa S, et al. HER-2 expression in canine morphologically normal, hyperplastic and neoplastic mammary tissues and its correlation with the

clinical outcome. Res Vet Sci. 2013; 94(2):299–305. https://doi.org/10.1016/j.rvsc.2012.09.016 PMID: 23141215

19. Burrai G, Tanca A, De Miglio M, Abbondio M, Pisanu S, Polinas M, et al. Investigation of HER2 expression in canine mammary tumors by antibody-based, transcriptomic and mass spectrometry analysis: is the dog a suitable animal model for human breast cancer? Tumor Biol. 2015; 36(11):9083–91.
20. Wang F, Flanagan J, Su N, Wang LC, Bui S, Nielson A, et al. RNAscope: a novel in situ RNA analysis platform for formalin-fixed, paraffin-embedded tissues. J Mol Diagn. 2012; 14(1):22–9. https://doi.org/10.1016/j.jmoldx.2011.08.002 PMID: 22166544
21. Kim KK, Seung BJ, Kim D, Park HM, Lee S, Song DW, et al. Whole-exome and whole-transcriptome sequencing of canine mammary gland tumors. Sci Data. 2019; 6(1):147. https://doi.org/10.1038/s41597-019-0149-8 PMID: 31413331
22. Seung BJ, Lim HY, Shin JI, Kim HW, Cho SH, Kim SH, et al. CD204-Expressing Tumor-Associated Macrophages Are Associated With Malignant, High-Grade, and Hormone Receptor–Negative Canine Mammary Gland Tumors. Vet Pathol. 2018; 55(3):417–24. https://doi.org/10.1177/0300985817750457 PMID: 29343199
23. Wolff AC, Hammond MEH, Hicks DG, Dowsett M, McShane LM, Allison KH, et al. Recommendations for human epidermal growth factor receptor 2 testing in breast cancer: American Society of Clinical Oncology/College of American Pathologists clinical practice guideline update. Arch Pathol Lab Med. 2014; 138(2):241–56. https://doi.org/10.5858/arpa.2013-0953-SA PMID: 24099077
24. Müller BM, Kronenwett R, Hennig G, Euting H, Weber K, Bohmann K, et al. Quantitative determination of estrogen receptor, progesterone receptor, and HER2 mRNA in formalin-fixed paraffin-embedded tissue—a new option for predictive biomarker assessment in breast cancer. Diagn Mol Pathol. 2011; 20(1):1–10. https://doi.org/10.1097/PDM.0b013e3181e3630c PMID: 21326033
25. Schindelin J, Arganda-Carreras I, Frise E, Kaynig V, Longair M, Pietzsch T, et al. Fiji: an open-source platform for biological-image analysis. Nat Methods. 2012; 9(7):676–82. https://doi.org/10.1038/nmeth.2019 PMID: 22743772
26. De Chaumont F, Dallongeville S, Chenouard N, Hervé N, Pop S, Provoost T, et al. Icy: an open bioimage informatics platform for extended reproducible research. Nat Methods. 2012; 9(7):690–6. https://doi.org/10.1038/nmeth.2075 PMID: 22743774
27. Tsuboi M, Sakai K, Maeda S, Chambers JK, Yonezawa T, Matsuki N, et al. Assessment of HER2 Expression in Canine Urothelial Carcinoma of the Urinary Bladder. Vet Pathol. 2019; 56(3):369–76. https://doi.org/10.1177/0300985818817024 PMID: 30612533
28. Slamon DJ, Clark GM, Wong SG, Levin WJ, Ullrich A, McGuire WL. Human breast cancer: correlation of relapse and survival with amplification of the HER-2/neu oncogene. Science. 1987; 235(4785):177–82. https://doi.org/10.1126/science.3798106 PMID: 3798106
29. Seshadri R, Firgaira F, Horsfall D, McCaul K, Setlur V, Kitchen P. Clinical significance of HER-2/neu oncogene amplification in primary breast cancer. The South Australian Breast Cancer Study Group. J Clin Oncol. 1993; 11(10):1936–42.
30. Romond EH, Perez EA, Bryant J, Suman VJ, Geyer CE Jr, Davidson NE, et al. Trastuzumab plus adjuvant chemotherapy for operable HER2-positive breast cancer. N Engl J Med. 2005; 353(16):1673–84. https://doi.org/10.1056/NEJMoa052122 PMID: 16236738
31. Sassi F, Benazzi C, Castellani G, Sarli G. Molecular-based tumour subtypes of canine mammary carcinomas assessed by immunohistochemistry. BMC Vet Res. 2010; 6:5. https://doi.org/10.1186/1746-6148-6-5 PMID: 20109214
32. Damasceno KA, Ferreira E, Estrela-Lima A, de Oliveira Gamba C, Miranda FF, Alves MR, et al. HER-2 and EGFR mRNA expression and its relationship with versican in malignant matrix-producing tumors of the canine mammary gland. PloS One. 2016; 11(8):e0160419. https://doi.org/10.1371/journal.pone.0160419 PMID: 27490467
33. Vogel C, Marcotte EM. Insights into the regulation of protein abundance from proteomic and transcriptomic analyses. Nat Rev Genet. 2012; 13(4):227–32. https://doi.org/10.1038/nrg3185 PMID: 22411467
34. Buckley NE, Forde C, McArt DG, Boyle DP, Mullan PB, James JA, et al. Quantification of HER2 heterogeneity in breast cancer–implications for identification of sub-dominant clones for personalised treatment. Sci Rep. 2016; 6:23383. https://doi.org/10.1038/srep23383 PMID: 26996207
35. Wang Z, Portier BP, Gruver AM, Bui S, Wang H, Su N, et al. Automated quantitative RNA in situ hybridization for resolution of equivocal and heterogeneous ERBB2 (HER2) status in invasive breast carcinoma. J Mol Diagn. 2013; 15(2):210–9. https://doi.org/10.1016/j.jmoldx.2012.10.003 PMID: 23305906
36. Hsu WL, Huang HM, Liao JW, Wong ML, Chang SC. Increased survival in dogs with malignant mammary tumours overexpressing HER-2 protein and detection of a silent single nucleotide polymorphism in the canine HER-2 gene. Vet J. 2009; 180(1):116–23. https://doi.org/10.1016/j.tvjl.2007.10.013 PMID: 18061495

37. Kim JH, Im KS, Kim NH, Yhee JY, Nho WG, Sur JH. Expression of HER-2 and nuclear localization of HER-3 protein in canine mammary tumors: histopathological and immunohistochemical study. Vet J. 2011; 189(3):318–22. https://doi.org/10.1016/j.tvjl.2010.08.012 PMID: 20947393

38. Sakai K, Maeda S, Saeki K, Yoshitake R, Goto-Kishino Y, Nakagawa T, et al. ErbB2 Copy Number Aberration in Canine Urothelial Carcinoma Detected by a Digital Polymerase Chain Reaction Assay. Vet Pathol. 2020; 57(1):56–65. https://doi.org/10.1177/0300985819879445 PMID: 31640537

39. Press MF, Bernstein L, Thomas PA, Meisner LF, Zhou JY, Ma Y, et al. HER-2/neu gene amplification characterized by fluorescence in situ hybridization: poor prognosis in node-negative breast carcinomas. J Clin Oncol. 1997; 15(8):2894–904. https://doi.org/10.1200/JCO.1997.15.8.2894 PMID: 9256133

40. Starkey MP, Scase TJ, Mellersh CS, Murphy S. Dogs really are man's best friend—canine genomics has applications in veterinary and human medicine! Brief Funct Genomic Proteomic. 2005; 4(2):112–28. https://doi.org/10.1093/bfgp/4.2.112 PMID: 16102268

41. Paoloni M, Khanna C. Translation of new cancer treatments from pet dogs to humans. Nat Rev Cancer. 2008; 8(2):147–56. https://doi.org/10.1038/nrc2273 PMID: 18202698

42. Queiroga FL, Raposo T, Carvalho MI, Prada J, Pires I. Canine mammary tumours as a model to study human breast cancer: most recent findings. In Vivo. 2011; 25(3):455–65. PMID: 21576423

43. Mason NJ, Gnanandarajah JS, Engiles JB, Gray F, Laughlin D, Gaurnier-Hausser A, et al. Immunotherapy with a HER2-targeting Listeria induces HER2-specific immunity and demonstrates potential therapeutic effects in a phase I trial in canine osteosarcoma. Clin Cancer Res. 2016; 22(17):4380–90. https://doi.org/10.1158/1078-0432.CCR-16-0088 PMID: 26994144

44. Sakai K, Maeda S, Saeki K, Nakagawa T, Murakami M, Endo Y, et al. Anti-tumour effect of lapatinib in canine transitional cell carcinoma cell lines. Vet Comp Oncol. 2018; 16(4):642–49. https://doi.org/10.1111/vco.12434 PMID: 30246405